Organic & Biomolecular Chemistry

ROYAL SOCIETY OF CHEMISTRY

PAPER

View Article Online
View Journal | View Issue

Cite this: *Org. Biomol. Chem.*, 2021, **19**, 2744

A new synthetic protectin D1 analog 3-oxa-PD1$_{n\text{-}3\ DPA}$ reduces neuropathic pain and chronic itch in mice†

Jannicke Irina Nesman,[a] Ouyang Chen,[b] Xin Luo,[b] Ru-Rong Ji,[b] Charles N. Serhan[c] and Trond Vidar Hansen *[a]

Received 23rd October 2020,
Accepted 2nd March 2021

DOI: 10.1039/d0ob02136a

rsc.li/obc

The resolution of inflammation is a biosynthetically active process controlled by the interplay between oxygenated polyunsaturated mediators and G-protein coupled receptor-signaling pathways. These enzymatically oxygenated polyunsaturated fatty acids belong to distinct families of specialized pro-resolving autacoids. The protectin family of mediators has attracted an interest because of their potent pro-resolving and anti-inflammatory actions verified in several *in vivo* disease models. Herein, we present the stereoselective synthesis and biological evaluations of 3-oxa-PD1$_{n\text{-}3\ DPA}$, a protectin D1 analog. Results from mouse models indicate that the mediators protectin D1, PD1$_{n\text{-}3\ DPA}$ and the new analog 3-oxa-PD1$_{n\text{-}3\ DPA}$ all relieved streptozotocin-induced diabetic neuropathic pain at doses of 90 and 300 pmol, equivalent to 30 and 100 ng, respectively, following intrathecal (I.T.) injection. Of interest, at a low dose of only 30 pmol (10 ng; I.T.) only 3-oxa PD1$_{n\text{-}3\ DPA}$ was able to alleviate neuropathic pain, directly compared to vehicle controls. Moreover, using a chronic itch model of cutaneous T-cell lymphoma (CTCL), all three compounds at 300 pmol (100 ng) showed a significant reduction in itching for several hours. The biomolecular information on the structure-functions of the protectins and the new synthetic analog 3-oxa-PD1$_{n\text{-}3\ DPA}$ is of interest towards developing new immunoresolvents.

Introduction

The classical signs of inflammation are *rubor* (redness), *tumor* (swelling), *calor* (increased heat), *dolor* (pain) and *functio laesa* (loss of function). Pain is initially sensed by physical and chemical activation of sensory neurons named nociceptors.[1,2] Inflammatory mediators, resulting from the activation of the resident immune cells and microglia in the spinal cord and brain,[2] activate individual receptors expressed on nociceptors. This gives rise to inflammatory pain, and if unresolved, can progress into chronic pain.[3] Recent efforts have now established that unresolved neuroinflammation is an essential component in the development of chronic pain.[4] Neuroinflammation contributes to elimination of the initial cell injury caused by tissue repair, enabling homeostasis.[5] However, excessive and chronic inflammation is a leading cause of numerous inflammatory and neurological diseases.[6] Current pharmacotherapy options deliver inadequate and/or insufficient responses to acute and chronic pain and represent a significant unmet clinical need,[7] which is particularly true for the current opioid crisis in the USA.[8] Inflammation in skin diseases is also commonly associated with chronic itch, and effective treatment for this disorder is also lacking.[9]

New drugs resolving inflammatory and neuropathic pain are at the medicinal and bioorganic chemistry frontier.[10] The endogenous specialized pro-resolving mediators (SPMs), biosynthesized from ω-3 and ω-6 polyunsaturated fatty acids (PUFAs),[11] possesses potent pro-resolving and anti-inflammatory agonist actions.[12] SPMs are agonists towards individual G-protein coupled receptors (GPCRs)[13] and are attractive leads for the development of remedies and new treatment strategies against acute and chronic pain.[4,14] Earlier, endogenous mediators have been used as lead compounds in medicinal chemistry programs towards the development of new therapeutics targeting neuroinflammation and resolution of chronic pain.[15] Anandamide (**1**)[16] and protectin D1 (PD1) (**2**),[17] also denoted neuroprotectin D1 (NPD1) when isolated from neural cells,[18] are examples of such leads (Fig. 1).[3,15]

[a]*Department of Pharmacy, Section for Pharmaceutical Chemistry, University of Oslo, PO Box 1068 Blindern, N-0316 Oslo, Norway. E-mail: t.v.hansen@farmasi.uio.no*
[b]*Center for Translational Pain Medicine, Department of Anesthesiology, Duke University Medical Center, Durham, NC 27710, USA*
[c]*Center for Experimental Therapeutics and Reperfusion Injury, Department of Anesthesiology, Perioperative and Pain Medicine, Hale Building for Transformative Medicine, Brigham and Women's Hospital and Harvard Medical School, Boston, Massachusetts, 02115, USA*

†Electronic supplementary information (ESI) available. See DOI: 10.1039/d0ob02136a

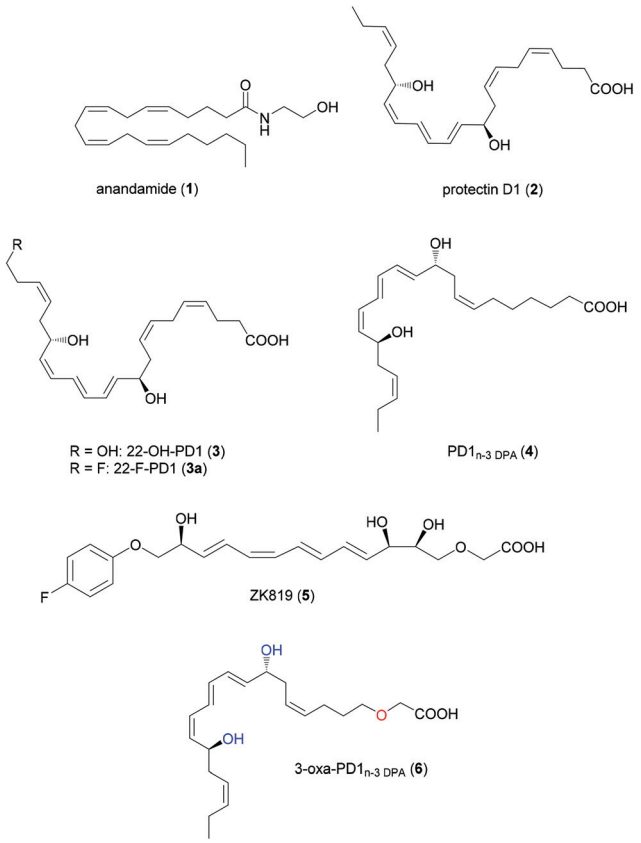

Fig. 1 Structures of anandamide (**1**), protectins (**2–4**), ZK819 (**5**) and the new analog 3-oxa-PD1$_{n\text{-}3\ DPA}$ (**6**).

As of today, arachidonic acid derived **1** has been the target of several research programs where structure–activity relationship studies targeting the CB_1 and the CB_2 cannabinoid receptors are reported.[16] The docosahexaenoic acid (DHA) derived and endogenously biosynthesized product **2** [10,11,24] displays attractive features as a lead compound and biomolecular template with an EC_{50}-value of ~1 nM and K_d-value of ~31 pmol mg^{-1} of cell protein,[19] showing great potential for drug discovery programs.[10c,20] Different analgesic properties are reported for DHA and its enzymatic biosynthesized oxygenated product **2**. Of note, DHA post-treatment showed no effects on chronic construction injury induced neuropathic pain[21] or bone fracture-induced postoperative pain at doses as high as 500 μg.[22] Of interest, pretreatment with DHA was reported to be effective[22] suggesting that DHA as a precursor needs to be enzymatically converted by cells and tissues to potent bioactive molecules. Along these lines, PD1 (**2**) shows potent neuroprotective properties when used as treatment in several experimental brain injury models.[21,22]

As noted above, SPMs are selective agonists towards GPCRs.[10,13] In 2018, Ji and co-workers reported that PD1 (**2**) is a potent agonist for GPR37.[23] Activation of GPR37 by this SPM **2** results in escalated levels of intracellular Ca^{2+} concentrations, leading to enhanced macrophage phagocytosis, which is a hallmark of a successful pro-resolution process.[24]

These observations support that PD1 (**2**) is a potential lead endogenous structure for resolution pharmacology.[10c] Fatty acids *in vivo*, including some SPMs *i.e.* lipoxin A_4,[25] can undergo secondary metabolism, including α-, β- and ω-omega oxidation processes that are organ, species and location dependent.[11,26] In order to avoid such catabolic oxidative degradation processes, the analog ZK819 was designed and synthesized (Fig. 1).[25] *In vivo* studies revealed that ZK819 exhibited enhanced chemical and metabolic stability and showed potent anti-inflammatory activity.[25] The ω-omega oxidation metabolite of PD1 (**2**) is 22-OH-PD1 (**3**),[27] which exhibited low nanomolar pro-resolution and anti-inflammatory bioactions, see Fig. 1. Similar bioactions were also observed for the synthetic analog 22-F-PD1 (**3a**)[28] and PD1$_{n\text{-}3\ DPA}$ (**4**),[29] where the latter is a congener of **2** biosynthesized from n-3 docosapentaenoic acid (n-3 DPA).[30] Of interest, Sala and colleagues reported recently that PD1 (**2**) undergoes rapid hepatic β-oxidative metabolism.[26b] Moreover, it was recently reported that 3-oxa n-3 DPA,[31] a β-oxidation resistant mimic of the parent PUFA n-3 DPA, was a substrate for the key enzyme 15-lipoxygenase (LOX) in the biosynthesis of the protectins.[32] PD1$_{n\text{-}3\ DPA}$ (**5**) displays interesting biological activities.[33] Hence, the synthetic analog 3-oxa-PD1$_{n\text{-}3\ DPA}$ (**6**) (Fig. 1) was stereoselectively prepared by total organic synthesis and subjected to *in vivo* biological evaluations in mouse models of pain and itch.

Results and discussion

Synthesis

The synthetic strategy towards 3-oxa-PD1$_{n\text{-}3\ DPA}$ (**6**) was based on our earlier reports.[27,28,34] In brief, starting from commercially available lactone **7** as the starting material, aldehyde **8** was reacted in a *Z*-selective Wittig reaction with the pre-formed ylide of triphenyl(propyl)phosphonium bromide (**9**) to produce alkyne **10** over 5 steps (Scheme 1).[35]

Next, aldehyde **11** was prepared over five steps using literature protocols.[36] Then, following treatment of commercial 4-ethoxy-4-oxobutyl-triphenylphosphonium bromide (**12**) with NaHMDS, dropwise addition of aldehyde **11** provided ethyl ester **13** as one stereoisomer in 58% yield after chromatographic purification. Ethyl ester **13** was reduced using DIBAL-H and the resulting alcohol **14** was further reacted with

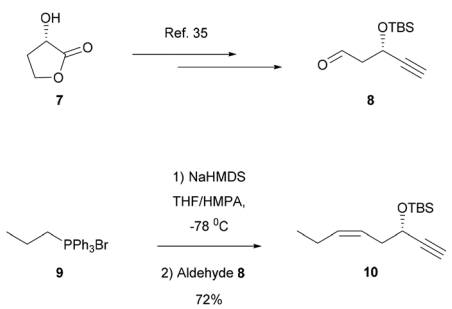

Scheme 1 Synthesis of aldehyde **8** and alkyne **10**.

tert-butyl bromoacetate **15** under phase transfer conditions to afford *tert*-butyl ester **16**. The vinylic bromide in **16** was reacted with alkyne **10** in a Sonogashira coupling reaction ($Pd(PPh_3)_4$, CuI, Et_2NH) that afforded **17**. Removal of the two TBS-groups was achieved with TBAF in THF to afford diol **18** in 72% yield over the two steps. Next, a protocol reported by Näf and co-workers[37] was applied, that provided a concomitant reduction of the alkyne functionality and hydrolysis of the *tert*-butyl ester, to give 3-oxa-$PD1_{n\text{-}3\ DPA}$ (**6**). Unfortunately, this provided only 10% of satisfactory chemical pure **6** after careful purification by chromatography. However, submitting the alkyne **18** to the Näf protocol and reacting the resulting crude acid with TMS-diazomethane, afforded the methyl ester of 3-oxa-$PD1_{n\text{-}3\ DPA}$ (**19**). Purification by chromatography provided **19** as one isomer in high chemical purity (>98%, HPLC analysis) and in 67% yield over the two steps (Scheme 2). Of note, data for the synthetic material of **2**, **3** and **4** have been matched earlier and individually with data, obtained from endogenous materials, using LC/MS-MS MRM and UV experiments.[27,29,34] The *Z* or *E* geometry for each of the double bonds in **6** was set by combining data from one and two-dimensional NMR spectroscopy. The ^1H–^1H COSY spectrum was used for assigning vicinal signals for both of the two isolated *Z*-olefins and the *E*,*E*,*Z*-triene moiety. In particular, the signals at 6.52 ppm (dd, 1H, J = 13.5, 11.7 Hz) and 6.07 ppm (t, 1H, J = 11.1 Hz) were diagnostic for the two *Z*-double bonds (ESI†). The NMR data for synthetic analog **6** was found to be in good agreement with literature for the natural occurring protectins **2–4**[27,28,29,32e–g,34] and the synthetic analog **5**[28] (Fig. 1). Furthermore, the UV-data obtained for the synthetic analog **6** (λ_{max} = 271 nm, shoulders at 261 and 282 nm (MeOH), ESI†) are in agreement with a *E*,*E*, *Z*-triene configuration present in protectins **2–4**[27,29,30a,32e–g] and the analog **5**.[28] For the *E*,*E*,*E*-triene configured stereoisomer of protectin D1 (**2**), the λ_{max} (MeOH) was observed at 269 nm.[32e] As for other protectins,[27–29,32–34] hydrolysis to the free acid **6** was performed just prior to biological evaluations.

Biological evaluations

Diabetic neuropathy is a major cause of neuropathic pain.[38] In the first study, a model for diabetic neuropathic pain was induced with intraperitoneal injection (I.P.) of streptozocin (STZ, 75 mg kg^{-1}) and utilized for behavioral testing. One week after the STZ treatment, mice developed a cardinal feature of neuropathic pain, mechanical allodynia, as revealed by a reduction in paw withdrawal threshold, compared to the baseline (BL, Fig. 2). After the validation of the successful development of neuropathic pain in all the STZ-treated mice, we further treated these mice with vehicle (PBS), PD1 (**2**), $PD1_{n\text{-}3\ DPA}$ (**5**), and 3-oxa-$PD1_{n\text{-}3\ DPA}$ (**6**) by intrathecal injection (I.T., 30), 90, and 300 pmol in 10 μl (Fig. 2A–C). We assessed paw withdrawal threshold at 1 hour, 3 hours, and 5 hours after the injections using von Frey test. Fig. 2A shows that at the lowest dose (30 pmol), only 3-oxa-$PD1_{n\text{-}3\ DPA}$ (**6**) was able to produce a transient reversal (at 1 hour time point) of STZ-induced neuro-

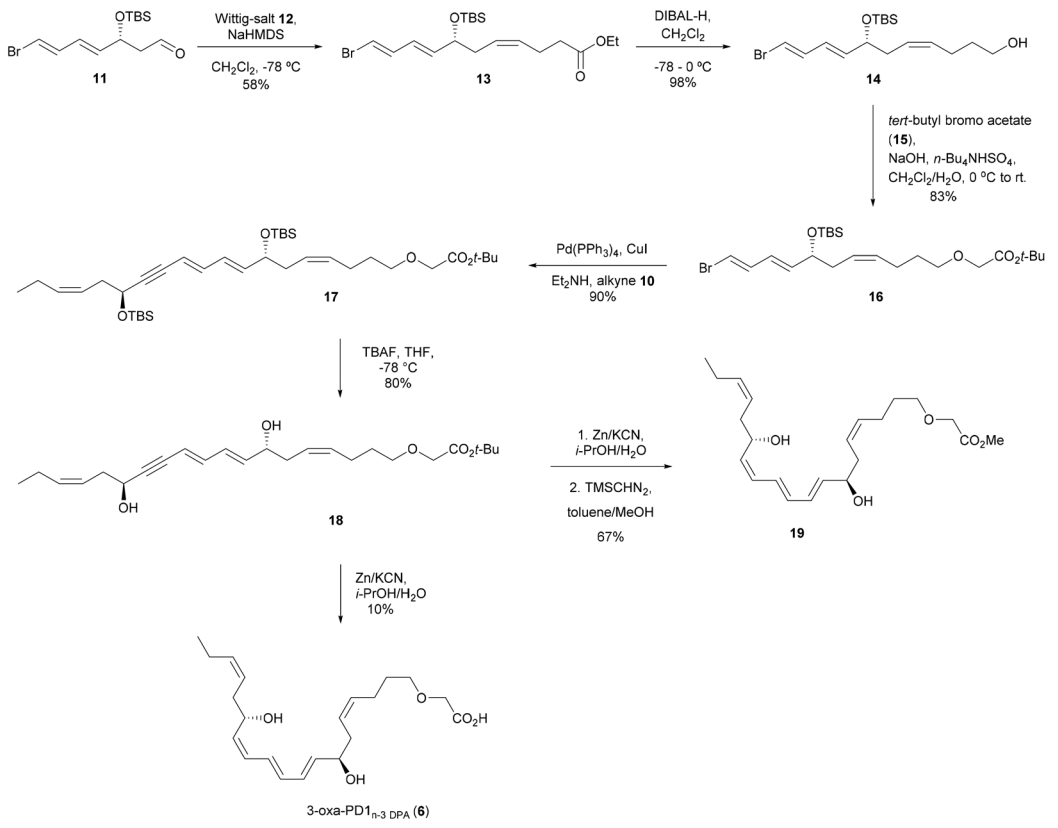

Scheme 2 Synthesis of 3-oxa-$PD1_{n\text{-}3\ DPA}$ (**6**) and its methyl ester **19**.

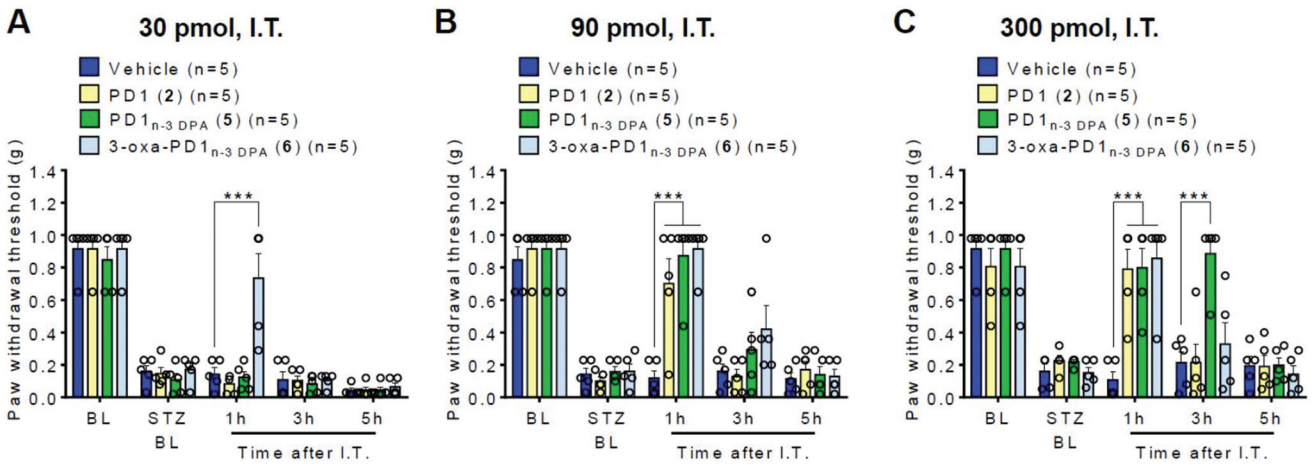

Fig. 2 Evaluations of streptozocin (STZ) induced neuropathic pain (mechanical allodynia) in mice mediated by 30 pmol (10 ng) (A), 90 pmol (30 ng) (B) and 300 pmol (100 ng) (C) of each of PD1 (**2**), $PD1_{n\text{-}3\ DPA}$ (**5**) and 3-oxa-$PD1_{n\text{-}3\ DPA}$ (**6**) using vehicle (PBS) as control. Compounds were delivered by intrathecal (I.T.) injection. ***$P < 0.001$, two-way ANOVA followed by *post-hoc* Bonferroni test. $n = 5$ male mice per treatment group. Each circle represents one animal. Neuropathic pain was assessed by paw withdrawal threshold using von Frey hairs. BL, baseline.

pathic pain (mechanical allodynia) compared to vehicle group ($P < 0.001$, Fig. 2A). Notably, vehicle had no effect on mechanical sensitivity (Fig. 2A–C). At a higher dose (90 pmol), PD1 (**2**), $PD1_{n\text{-}3\ DPA}$ (**5**) and 3-oxa-$PD1_{n\text{-}3\ DPA}$ (**6**) all significantly alleviated the neuropathic pain symptom mechanical allodynia at one hour ($P < 0.001$, *vs.* vehicle, Fig. 2B). At the highest dose (300 pmol), each of the three compounds significantly reduced the STZ-induced mechanical allodynia at one hour ($P < 0.001$, *vs.* vehicle, Fig. 2C). Of note, $PD1_{n\text{-}3\ DPA}$ (**5**) appears to possess some protection after three hours, but this effect disappears after an additional two hours (Fig. 2C).

Cutaneous T-cell lymphomas (CTCL) are among the common skin cancers, and those patients with CTCL frequently suffer from severe chronic itching.[39] Hence, we recently introduced a mouse model of lymphoma-associated chronic itch in immune deficient mice.[40] In the second *in vivo* study, mice were inoculated with lymphoma cells. In the CTCL model, itch behavior (scratching) developed at 20 days and maintained for 60 days.[40] In those mice that developed chronic itch, we treated them with vehicle (PBS), and 300 pmol of PD1 (**2**), $PD1_{n\text{-}3\ DPA}$ (**5**) and 3-oxa-$PD1_{n\text{-}3\ DPA}$ (**6**) to investigate the effect of each compound on relieving the unpleasant sensation provoking the desire to scratch at one hour, three hours, and five hours after the treatment. Following intraperitoneal injection (I.P., 300 pmol or 100 ng in 0.1 ml) of each compound, no effects of the protectin compounds on the scratch numbers were observed over five hours, as compared to the vehicle group (Fig. 3A). However, using intrathecal injection (I.T.) of 300 pmol each of **2**, **5** and **6** produced a significant reduction in the scratch number at one hour ($P < 0.001$, *vs.*

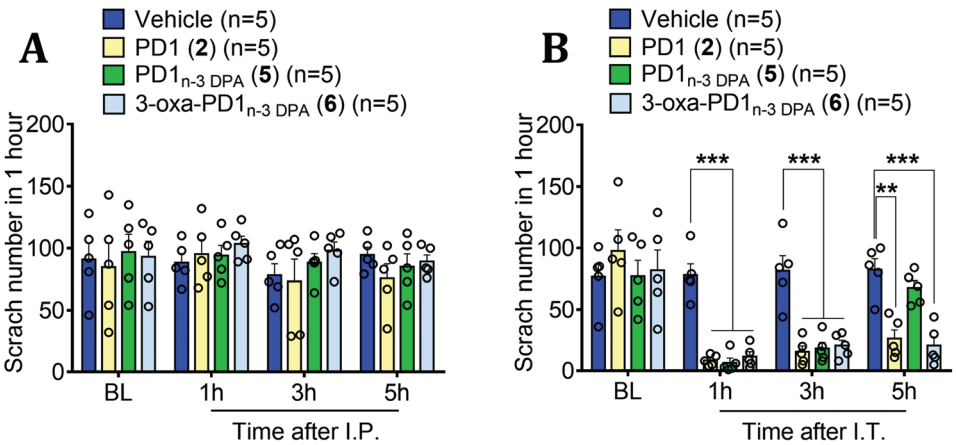

Fig. 3 Evaluations of cutaneous T-cell lymphoma (CTCL) induced chronic itch in mice treated by 300 pmol (100 ng) of each of PD1 (**2**), $PD1_{n\text{-}3\ DPA}$ (**5**) and 3-oxa-$PD1_{n\text{-}3\ DPA}$ (**6**) using vehicle (PBS) as control. (A) Compounds were delivered by intraperitoneal injection (I.P., 0.1 ml, 300 pmol). (B) Compounds were delivered by intrathecal (I.T., 10 μl, 300 pmol) injection. **$P < 0.01$, ***$P < 0.001$, two-way ANOVA followed by *post-hoc* Bonferroni test. $n = 5$ mice (3 males and 2 females) per treatment group. Each circle represents one animal. Chronic itch was assessed by number of scratches per hour. BL, baseline.

vehicle, Fig. 3B). Interestingly, the effects from each of the compounds remained after an additional two hours. For SPM **2** and our synthetic analog **6**, a reduction in the scratch number compared to control was also observed after 5 hours ($P < 0.01$, *vs.* vehicle, Fig. 3B). However, SPM **5** gave a different outcome, as there was apparently no apparent relief from itching after five hours (Fig. 3B). These initial and preliminary results demonstrate *in vivo* efficacy of the protectins **2** and **5** as well as the analog **6** that merit further biological evaluations.

Conclusions

The SPMs are among the most interesting small and naturally occurring molecules currently undergoing investigations towards clinical development of new anti-inflammatory and pro-resolving drugs with a novel general mechanism of action, namely as agonists stimulating resolution of local inflammation.[10,15] In the present report, the design and stereoselective synthesis of a novel protectin D1 analog coined 3-oxa-$PD1_{n\text{-}3\ DPA}$ (**6**) is presented. The total synthesis gave multi milligram quantities of **6** and its corresponding methyl ester **19**, available for further studies. The synthetic analog 3-oxa-$PD1_{n\text{-}3\ DPA}$ (**6**) showed equal potency as PD1 (**2**) and $PD1_{n\text{-}3\ DPA}$ (**5**) at 30–300 pmol dose range in reducing neuropathic pain as well as chronic itch following intrathecal injection in animal models, and thus retained the potent bioactions of these two SPMs. Notably, at the lowest dose (30 pmol per I.T.), only the synthetic analog 3-oxa-$PD1_{n\text{-}3\ DPA}$ (**6**) exhibited analgesic action in a mouse model of diabetic neuropathy. The biological effects depended on the route of administration. Worthy of note, I.T. injection of analog **6** could target cells in both dorsal root ganglion and spinal cord.[41] Further biological evaluations of SPMs **2**, **5** and analog **6** are currently ongoing and will be reported separately. However, the results presented contribute to new knowledge on the structure–function and biomolecular properties of the specialized pro-resolving lipid mediators.

Experimental section

General information

Unless otherwise stated, all commercially available reagents and solvents were used in the form in which they were supplied without any further purification. The stated yields are based on isolated material. Diastereomeric ratios reported have not been validated by calibration, see Wernerova and Hudlicky for discussions and guidelines.[42] All reactions were performed under an argon atmosphere using Schlenk techniques. Reaction flasks were covered with aluminum foil during reactions and storage to minimize exposure to light. Thin layer chromatography was performed on silica gel 60 F_{254} aluminum-backed plates fabricated by Merck. Flash column chromatography was performed on silica gel 60 (40–63 μm) produced by Merck. NMR spectra were recorded on a Bruker AVI600, Bruker AVII400 or a Bruker DPX300 spectrometer at 600 MHz, 400 MHz or 300 MHz respectively for ^{1}H NMR and at 150 MHz, 100 MHz or 75 MHz respectively for ^{13}C NMR. Coupling constants (J) are reported in hertz and chemical shifts are reported in parts per million (δ) relative to the central residual protium solvent resonance in ^{1}H NMR ($CDCl_3$ = δ 7.26, DMSO-d_6 = δ 2.50 and MeOD = δ 3.31) and the central carbon solvent resonance in ^{13}C NMR ($CDCl_3$ = δ 77.00 ppm, DMSO-d_6 = δ 39.43 and MeOD = δ 49.00). Optical rotations were measured using a 0.7 mL cell with a 1.0 dm path length on an Anton Paar MCP 100 polarimeter. Mass spectra were recorded at 70 eV on a Micromass Prospec Q or Micromass QTOF 2 W spectrometer using ESI as the method of ionization. High-resolution mass spectra were recorded at 70 eV on a Micromass Prospec Q or Micromass QTOF 2 W spectrometer using ESI as the method of ionization. HPLC-analyses were performed using a C18 stationary phase (Eclipse XDB-C18, 4.6 × 250 mm, particle size 5 μm, from Agilent Technologies), applying the conditions stated. The UV/Vis spectra were recorded using an Agilent Technologies Cary 8485 UV-VIS spectrophotometer using quartz cuvettes.

Ethyl (*R*,4*Z*,8*E*,10*E*)-11-bromo-7-((*tert*-butyldimethylsilyl)oxy) undeca-4,8,10-trienoate (13)

The commercially available Wittig salt **12** (0.399 g, 0.872 mmol, 1.00 eq.) in CH_2Cl_2 (15 mL) was added NaHMDS dropwise (0.6 M in toluene, 1.4 mL, 0.960 eq.) at −78 °C. The mixture turned from clear to yellow in color upon addition. Over 1 h, this solution was warmed to rt and then re-cooled to −78 °C followed by dropwise addition of aldehyde **11** (279 mg, 0.878 mmol, 1.00 eq.). The reaction mixture was slowly allowed to warm to rt in a dry ice/acetone bath over night. After 24 h, the dark green colored mixture was quenched with phosphate buffer (15 mL, pH = 7.0). The phases were separated and the aq. phase was extracted with CH_2Cl_2 (3 × 6.0 mL). The combined organic layer was dried and the solvent evaporated. The crude ethyl ester was added hexane (25 mL) and the precipitate was removed by filtration through a pad of Celite® that was washed twice with 5% EtOAc in hexane (5.0 mL). The residue was purified by column chromatography on silica gel (2–5% EtOAc in hexane) to give the title compound **13** as a clear oil. Yield: 201 mg (58%). All spectroscopic and physical data were inn agreement with those reported in the literature.[43] $[\alpha]_D^{20}$ = −11.0 (c = 0.37, $CHCl_3$); ^{1}H NMR (400 MHz, DMSO-d_6) δ 6.80 (dd, J = 13.4, 10.7 Hz, 1H), 6.64 (d, J = 13.4 Hz, 1H), 6.15 (ddd, J = 15.3, 10.7, 1.2 Hz, 1H), 5.82 (dd, J = 15.3, 6.0 Hz, 1H), 5.46–5.31 (m, 2H), 4.20 (q, J = 5.9 Hz, 1H), 4.04 (q, J = 7.1 Hz, 2H), 2.34–2.28 (m, 2H), 2.27–2.15 (m, 4H), 1.17 (t, J = 7.1 Hz, 3H), 0.86 (s, 9H), 0.03 (s, 3H), 0.01 (s, 3H); ^{13}C NMR (101 MHz, DMSO-d_6) δ 172.3, 137.9, 136.9, 129.7, 126.4, 126.1, 109.2, 71.9, 59.7, 35.5, 33.4, 25.7(3C), 22.6, 17.9, 14.1, −4.6, −4.8; TLC (hexane/EtOAc 95 : 5, visualized by UV and CAM-stain) R_f = 0.35.

(*R*,4*Z*,8*E*,10*E*)-11-Bromo-7-((*tert*-butyldimethylsilyl)oxy)undeca-4,8,10-trien-1-ol (14)

Ethyl ester **13** (492 mg, 1.18 mmol, 1.00 eq.) was dissolved in dry CH_2Cl_2 (65 mL) and cooled to −78 °C followed by dropwise

addition of DIBAL-H (1.0 M in DCM, 3.0 mL, 2.54 eq.). The reaction mixture was stirred for one hour before it was warmed to 0 °C and stirred for an additional 2 h. The reaction was judged complete by TLC analysis and added a sat. aq. solution of Rochelle salt (40 mL) and stirred vigorously for 1.5 hours. Next, the phases were separated and the aq. phase extracted with CH_2Cl_2 (3 × 20 mL). The combined organic extracts were washed with brine (50 mL), dried (Na_2SO_4), filtered and then concentrated *in vacuo*. The crude ester was purified by filtration through a plug of silica (hexane/EtOAc 7 : 3) to give the desired alcohol **14** as a clear oil. Yield: 440 mg (98%). $[\alpha]_D^{25}$ = +14.4 (*c* = 0.5, MeOH); ^{1}H NMR (400 MHz, $CDCl_3$) δ 6.69 (dd, *J* = 13.4, 10.9 Hz, 1H), 6.28 (d, *J* = 13.5 Hz, 1H), 6.14–6.02 (m, 1H), 5.72 (dd, *J* = 15.2, 5.8 Hz, 1H), 5.52–5.36 (m, 2H), 4.16 (q, *J* = 5.8 Hz, 1H), 3.64 (t, *J* = 6.5 Hz, 2H), 2.36–2.19 (m, 2H), 2.11 (q, *J* = 7.0 Hz, 2H), 1.62 (p, *J* = 6.8 Hz, 2H), 0.89 (s, 9H), 0.05 (s, 3H), 0.03 (s, 3H); ^{13}C NMR (101 MHz, $CDCl_3$) δ 138.0, 137.1, 131.2, 126.7, 125.9, 108.3, 72.6, 62.6, 36.2, 32.6, 26.0(3C), 23.9, 18.4, −4.4, −4.6; TLC (hexane/EtOAc 8 : 2, visualized by UV and $KMnO_4$-stain) R_f = 0.41; HRMS (ESI): calculated for $C_{17}H_{31}BrNaO_2Si$ $[M + Na]^+$: 397.1169, found: 397.1169.

tert-Butyl 2-(((*R*,4*Z*,8*E*,10*E*)-11-bromo-7-((*tert*-butyldimethylsilyl)oxy)undeca-4,8,10-trien-1-yl)oxy)acetate (16)

Alcohol **14** (75 mg, 0.200 mmol, 1.00 eq.) was dissolved in CH_2Cl_2 (5.0 mL) followed by addition of *n*-Bu_4NHSO_4 (68 mg, 0.200 mmol, 1.00 eq.) and *tert*-butyl bromoacetate (390 mg, 2.00 mmol, 10.0 eq.). The vigorously stirred mixture was cooled to 0 °C and added an aq. solution of NaOH (50% w/v, 5.0 mL). The resulting biphasic reaction mixture was stirred for 24 h and allowed to warm to ambient temperature over the stated time. Water (10 mL) and CH_2Cl_2 (10 mL) was added and the phases were separated. The aq. phase was extracted with CH_2Cl_2 (4 × 5.0 mL). The combined organic extracts were dried (Na_2SO_4), filtered, and concentrated *in vacuo*. The crude product was purified by column chromatography on silica gel (hexane/EtOAc 95 : 5) to give the title compound **16** as a clear oil. Yield: 81 mg (83%). $[\alpha]_D^{25}$ = −16.0 (*c* = 0.11, $CHCl_3$); ^{1}H NMR (400 MHz, $CDCl_3$) δ 6.73–6.61 (m, 1H), 6.27 (d, *J* = 13.5 Hz, 1H), 6.08 (ddd, *J* = 15.3, 10.9, 0.7 Hz, 1H), 5.71 (dd, *J* = 15.2, 5.8, 1H), 550–5.33 (m, 2H), 4.14 (q, *J* = 6.0 Hz, 1H), 3.94 (s, 2H), 3.50 (t, *J* = 6.6 Hz, 2H), 2.32–2.18 (m, 2H), 2.10 (q, *J* = 7.3 Hz, 2H), 1.66 (p, *J* = 6.8 Hz, 2H), 1.48 (s, 9H), 0.88 (s, 9H), 0.04 (s, 3H), 0.02 (s, 3H); ^{13}C NMR (101 MHz, $CDCl_3$) δ 169.9, 138.1, 137.1, 131.2, 126.6, 125.7, 108.3, 81.6, 72.6, 71.2, 68.9, 36.2, 29.6, 28.3(3C), 26.0(3C), 24.1, 18.4, −4.4, −4.6; TLC (hexane/EtOAc 95 : 5, visualized by UV and $KMnO_4$-stain) R_f = 0.28; HRMS (ESI): calculated for $C_{23}H_{41}BrNaO_4Si$ $[M + Na]^+$: 511.1850, found: 511.1850.

tert-Butyl 2-(((4*Z*,7*R*,8*E*,10*E*,14*S*,16*Z*)-7,14-bis((*tert*-butyldimethylsilyl)oxy)nonadeca-4,8,10,16-tetraen-12-yn-1-yl)oxy)acetate (17)

Vinyl bromide **16** (256 mg, 0.523 mmol, 1.00 eq.) was added $Pd(PPh_3)_4$ (19.0 mg, 16.4 μmol, 3.00 mol%) and the flask evacuated and filled with argon. Et_2NH (1.0 mL) and benzene (0.45 mL) were added, and the reaction was stirred for 45 min in the dark. CuI (6.00 mg, 0.0315 mmol, 6 mol%) dissolved in a minimal amount of Et_2NH was added, followed by dropwise addition of alkyne **11** (130 mg, 0.545 mmol, 1.04 eq.) in Et_2NH (1.0 mL). After 26 h of stirring at ambient temperature, the reaction was quenched with sat. aq. NH_4Cl (10 mL). Et_2O (10 mL) was added, and the phases were separated. The aq. phase was extracted with Et_2O (2 × 10 mL), and the combined organic layers were dried (Na_2SO_4), filtered, and the solvent evaporated. The crude product was purified by column chromatography on silica gel (hexane/EtOAc, 98 : 2) to afford the title compound **17** as a clear oil. Yield: 305 mg (90%). $[\alpha]_D^{20}$ = −21.8 (*c* = 0.40, $CHCl_3$); ^{1}H NMR (400 MHz, $CDCl_3$) δ 6.50 (dd, *J* = 15.5, 10.9 Hz, 1H), 6.18 (dd, *J* = 15.2, 10.9 Hz, 1H), 5.75 (dd, *J* = 15.2, 6.0 Hz, 1H), 5.61–5.28 (m, 5H), 4.50–4.42 (m, 1H), 4.17 (q, *J* = 6.0 Hz, 1H), 3.94 (s, 2H), 3.50 (t, *J* = 6.6 Hz, 2H), 2.43 (t, *J* = 6.6 Hz, 2H), 2.32–2.17 (m, 2H), 2.15–1.99 (m, 4H), 1.66 (p, *J* = 6.8 Hz, 2H), 1.48 (s, 9H), 0.96 (s, 3H), 0.90 (s, 9H), 0.88 (s, 9H), 0.13 (s, 3H), 0.11 (s, 3H), 0.04 (s, 3H), 0.02 (s, 3H); ^{13}C NMR (101 MHz, $CDCl_3$) δ 169.9, 141.2, 139.3, 134.4, 131.1, 128.6, 125.9, 124.1, 110.7, 93.4, 83.5, 81.6, 72.9, 71.2, 69.0, 63.7, 36.8, 36.3, 29.6, 28.3(3C), 26.0(3C), 26.0(3C), 24.1, 20.9, 18.5, 18.4, 14.4, −4.3(2C), −4.6, −4.8; TLC (hexane/EtOAc 95 : 5, visualized by UV and $KMnO_4$-stain) R_f = 0.32; HRMS (ESI): calculated for $C_{37}H_{66}NaO_5Si_2$ $[M + Na]^+$: 669.4341, found: 669.4340.

tert-Butyl 2-(((4*Z*,7*R*,8*E*,10*E*,14*S*,16*Z*)-7,14-dihydroxynonadeca-4,8,10,16-tetraen-12-yn-1-yl)oxy)acetate (18)

TBAF (1.0 M in THF, 1.2 mL, 1.20 mmol, 5.11 eq.) was added to a solution of silyl ether **17** (152 mg, 0.235 mmol, 1.00 eq.) in THF (2.5 mL) at −78 °C. The reaction was stirred for 21 h before it was quenched with phosphate buffer (pH = 7.0, 4.0 mL). Brine (15 mL) and EtOAc (15 mL) were added, and the phases were separated. The aq. phase was extracted with EtOAc (2 × 10 mL), and the combined organic layer was dried (Na_2SO_4) and filtered before the solvent was evaporated. The crude product was purified by column chromatography on silica gel (hexane/EtOAc, 7 : 3) to afford the title compound **18** as a clear oil. Yield: 78 mg (80%). $[\alpha]_D^{20}$ = −8.37 (*c* = 0.43, MeOH); ^{1}H NMR (400 MHz, MeOD) δ 6.54 (dd, *J* = 15.5, 10.8 Hz, 1H), 6.28 (dd, *J* = 15.2, 10.8 Hz, 1H), 5.82 (dd, *J* = 15.2, 6.3 Hz, 1H), 5.66 (d, *J* = 15.5 Hz, 1H), 5.57–5.38 (m, 4H), 4.41 (td, *J* = 6.7, 1.9 Hz, 1H), 4.13 (q, *J* = 6.5 Hz, 1H), 3.96 (s, 2H), 3.50 (t, *J* = 6.4 Hz, 2H) 2.50–2.37 (m, 2H), 2.35–2.25 (m, 2H), 2.18–2.03 (m, 4H), 1.68–1.60 (m, 2H), 1.48 (s, 9H), 0.98 (t, *J* = 7.5 Hz, 3H); ^{13}C NMR (101 MHz, MeOD) δ 171.7, 142.5, 139.9, 135.3, 132.3, 130.3, 126.7, 124.7, 111.7, 93.8, 84.3, 82.7, 72.8, 72.0, 69.6, 63.3, 36.9, 36.2, 28.4(3C), 24.9, 21.7, 14.6; TLC (hexane/EtOAc 7 : 3, visualized by UV and $KMnO_4$-stain) R_f = 0.21; HRMS (ESI): calculated for $C_{25}H_{38}NaO_5$ $[M + Na]^+$: 441.2611, found: 441.2611.

2-(((4*Z*,7*R*,8*E*,10*E*,12*Z*,14*S*,16*Z*)-7,14-Dihydroxynonadeca-4,8,10,12,16-pentaen-1-yl)oxy)acetic acid (6)

The analog 3-oxa-PD1$_{n\text{-}3\ DPA}$ (**6**) was prepared by following the protocol reported by Näf and co-workers.[37] A mixture of alkyne

18 (48.0 mg, 0.115 mmol, 1.00 eq.), zinc powder (1.64 g, 25.1 mmol, 218 eq.) and potassium cyanide (110 mg, 1.69 mmol, 14.7 eq.) was added a solution of i-PrOH/H_2O (5.0 mL 1 : 1, pH = 7.0), and stirred at ambient temperature under protection of argon in the dark. After stirring for 26 h, the reaction mixture was filtered through a pad of Celite® and the pad washed with EtOAc (10 mL). Sat. aq. NH_4Cl (10 mL) was added to the filtrate and the phases were separated. The aq. phase was extracted with EtOAc (3 × 6.0 mL), and the combined organic layer was dried (Na_2SO_4), filtered, and the solvent evaporated. The crude product was repeatedly and carefully purified using a Biotage® Select purification system (Biotage® Sfär-C-18, 40–50% MeOH/3.3 mM AcOH, 6.0 mL min^{-1}) to give 4 mg (10%) of the title compound **6** as a pale yellow oil. ^{1}H NMR (600 MHz, MeOD) δ 6.52 (dd, J = 13.5, 11.7 Hz, 1H), 6.32–6.20 (m, 2H), 6.07 (t, J = 11.1 Hz, 1H), 5.75 (dd, J = 14.2, 6.1 Hz, 1H), 5.53–5.31 (m, 5H), 4.56 (q, J = 6.8 Hz, 1H), 4.12 (p, J = 6.5 Hz, 1H), 4.09 (s, 2H), 3.53 (t, J = 6.7 Hz, 2H), 2.40–2.24 (m, 3H), 2.23–2.17 (m, 1H), 2.13 (q, J = 7.3 Hz, 2H), 2.07 (p, J = 7.0 Hz, 2H), 1.67 (p, J = 7.0 Hz, 2H), 0.97 (t, J = 7.5 Hz, 3H); ^{13}C NMR (151 MHz, MeOD) δ 178.0, 138.0, 135.0, 134.9, 134.7, 132.3, 131.4, 130.6, 128.9, 126.7, 125.3, 73.1, 71.7, 71.0, 68.5, 36.4, 36.3, 30.3, 24.9, 21.7, 14.6; TLC (EtOAc/CH_2Cl_2/MeOH 6 : 5 : 4, visualized by UV and $KMnO_4$-stain) R_f = 0.2; HRMS (ESI): calculated for $C_{21}H_{32}NaO_5$ $[M + Na]^+$: 387.2142, found: 387.2142; UV-VIS: λ_{max} (MeOH) = 261, 271, 282 nm. The purity (>98%) was determined by HPLC analysis (Eclipse XDB-C18, MeOH/3.3 mM AcOH, 66 : 34, 1.0 mL min^{-1}); t_r = 16.8.

Methyl 2-(((4*Z*,7*R*,8*E*,10*E*,12*Z*,14*S*,16*Z*)-7,14-dihydroxynonadeca-4,8,10,12,16-pentaen-1-yl)oxy)acetate (19)

Methyl ester **19** was prepared by following the protocol reported by Näf and co-workers.[37] A mixture of alkyne **18** (48.0 mg, 0.115 mmol, 1.00 eq.), zinc powder (1.64 g, 25.1 mmol, 218 eq.) and potassium cyanide (110 mg, 1.69 mmol, 14.7 eq.) was added a solution of i-PrOH/H_2O (5.0 mL 1 : 1, pH = 7.0), and stirred at ambient temperature under protection of argon in the dark. After stirring for 26 h, the reaction mixture was filtered through a pad of Celite® and the pad washed with EtOAc (10 mL). Sat. aq. NH_4Cl (10 mL) was added to the filtrate and the phases were separated. The aq. phase was extracted with EtOAc (3 × 6.0 mL), and the combined organic layer was dried (Na_2SO_4), filtered, and the solvent evaporated, but not to dryness. The crude product was immediately added a solvent mixture of toluene/MeOH (3 : 2, 3.0 mL). Next, TMS-diazomethane (2.0 M in Et_2O, 0.1 mL, 1.30 eq.) was dropwise added to the crude product under rapid stirring until the yellow color persisted. After stirring for 45 min, the reaction was quenched with sat. aq. NH_4Cl (10 mL). The layers were separated and the aq. phase extracted with Et_2O (3 × 5.0 mL). The combined organic layer was evaporated, and the residue was purified by column chromatography on silica gel (hexane/EtOAc, 4 : 6 and drops of MeOH) to afford the title compound **19** as a clear oil. Yield: 31 mg (67% over the two steps); $[\alpha]_D^{25}$ = +30.6 (c = 0.081, MeOH); ^{1}H NMR (600 MHz, MeOD) δ 6.56–6.47 (m, 1H), 6.33–6.20 (m, 2H), 6.07 (t, J = 11.1 Hz, 1H), 5.75 (dd, J = 14.5, 6.5 Hz, 1H), 5.52–5.31 (m, 5H), 4.56 (q, J = 6.0 Hz, 1H), 4.13 (q, J = 6.5 Hz, 1H), 4.09 (s, 2H), 3.73 (s, 3H), 3.52 (t, J = 6.2 Hz, 2H), 2.41–2.24 (m, 3H), 2.24–2.17 (m, 1H), 2.14 (q, J = 7.2 Hz, 2H), 2.06 (p, J = 7.5 Hz, 2H), 1.65 (p, J = 7.1 Hz, 2H), 0.97 (t, J = 7.5 Hz, 3H); ^{13}C NMR (151 MHz, MeOD) δ 172.8, 138.1, 135.0, 134.8, 134.7, 132.1, 131.3, 130.6, 128.9, 126.8, 125.3, 73.1, 72.1, 68.9, 68.6, 52.2, 36.4, 36.3, 30.4, 24.8, 21.7, 14.6; TLC (hexane/EtOAc 4 : 6, visualized by UV and $KMnO_4$-stain) R_f = 0.43; HRMS (ESI): calculated for $C_{22}H_{34}NaO_5$ $[M + Na]^+$: 401.2298, found: 401.2298; UV-VIS: λ_{max} (MeOH) = 261, 271, 282 nm. The purity (>98%) was determined by HPLC analysis (Eclipse XDB-C18, MeOH/H_2O, 70 : 30, 1.0 mL min^{-1}); t_r = 15.2.

Biological experiments in animals

Hydrolysis of methyl ester **19** to the free acid **6** was performed just prior to biological evaluations as earlier reported.[34]

Animals

Wild-type CD1 mice were purchased from Charles River Laboratories, and NOD.CB-17-Prkdcscid mice (Stock #001303) were purchased from the Jackson Laboratory (Bar Harbor, Maine). Mice were group-housed on a 12-hour light/12-hour dark cycle at 22 ± 1 °C with free access to food and water at Duke University Animal Facilities. Animals were randomly assigned to each group. Two to five mice were housed in each cage. Adult mice (8–12 weeks old) of both sexes were used for behavioral experiments unless specified. All the animal experiments were approved by Institutional Animal Care Use Committee of Duke University and conducted in accordance with the National Institutes of Health Guide for the Care and Use of Laboratory Animals. Animal behaviors were tested blindly. For intrathecal injection, spinal cord puncture was made by a Hamilton microsyringe (Hamilton Company, Reno, Nevada) with a 30-G needle between the L5 and L6 level to deliver reagents (10 μl) to the cerebral spinal fluid.[44]

Evaluation of diabetic neuropathic pain

Diabetic neuropathic pain was induced *via* systemic injection of streptozotocin (STZ, Sigma, 75 mg kg^{-1}, I.P.). STZ was dissolved in saline solution (50 mg ml^{-1}). Neuropathic pain rapidly develops within 3 days after the STZ injection. For behavioral tests for mechanical sensitivity, mice were habituated to the testing environment daily for two days before von Frey tests. Mice were confined in boxes that are placed on an elevated metal mesh floor and their hindpaws were stimulated with a series of von Frey hairs (0.02–2.56 g, Stoelting). The calibrated von Frey hairs were presented perpendicularly to the plantar surface. We determined the 50% paw withdrawal threshold by Dixon's up-down method.[45] All of the behavioral tests were conducted between 9 : 00 am to 5 : 00 pm. One week after the STZ injection, mice were given intrathecal injection of PBS (vehicle) or doses of 30, 90 or 300 pmol (10, 30 or 100 ng) of PD1 (**2**), $PD1_{n\text{-}3\ DPA}$ (**5**) and 3-oxa-$PD1_{n\text{-}3\ DPA}$ (**6**).

Evaluation of itch in mouse CTCL xenograft model

Immune deficient mice (NOD.CB17-Prkdcscid) were used to produce xenograft model of cutaneous T-cell lymphoma (CTCL) as we previously described.[40] $CD4^+$ MyLa cell line was purchased from Sigma (Catalog # 95051032) for mouse inoculation. CTCL was generated *via* intradermal injection of $CD4^+$ Myla cells (1×10^5 cells per μl, 100 μl) on the nape of the neck under 2% isoflurane anesthesia.[46] The scratching behavior was video recorded for 60 min using Sony HDR-CX610 camera. The video was subsequently played back offline and the number of scratches in every 60 min was counted blindly. One month after the induction, mice were given intraperitoneal or intrathecal injection of PBS (vehicle) or 300 pmol (100 ng) of PD1 (**2**), $PD1_{n\text{-}3\ DPA}$ (**5**) and 3-oxa-$PD1_{n\text{-}3\ DPA}$ (**6**).

Statistical analyses

All data were expressed as mean ± SEM. Statistical analyses were completed with Prism GraphPad 6.0. Behavioral data were analyzed using two-way ANOVA followed by *post-hoc* Bonferroni test. The criterion for statistical significance was $P < 0.05$.

Conflicts of interest

Dr. Ru-Rong Ji is a consultant of Boston Scientific and also received a grant from the company. This activity is not related to this study.

Acknowledgements

T. V. H. is grateful for funding from the Research Council of Norway (FRIPRO-FRINATEK 230470) and The Department of Pharmacy is acknowledged for a scholarship to J. I. N. Duke University contributions are supported by Duke University Anesthesiology Research Funds. C. N. S. contributions are supported by NIH grant R01GM038765 (USA).

References

1 (*a*) A. I. Basbaum, D. M. Bautista, G. Scherrer and D. Julius, *Cell*, 2009, **139**, 267; (*b*) D. Julius and A. I. Basbaum, *Nature*, 2001, **413**, 203.
2 (*a*) C. J. Woolf and Q. Ma, *Neuron*, 2007, **55**, 353; (*b*) K. Inoue and M. Tsuda, *Nat. Rev. Neurosci.*, 2018, **19**, 138.
3 R.-R. Ji, Z. Z. Xu and Y. J. Gao, *Nat. Rev. Drug Discovery*, 2014, **13**, 533.
4 M. Matsuda, Y. Huh and R.-R. Ji, *J. Anesth.*, 2019, **33**, 131.
5 G. L. Bannenberg, N. Chiang, A. Ariel, M. Arita, E. Tjonahen, K. H. Gotlinger, S. Hong and C. N. Serhan, *J. Immunol.*, 2005, **174**, 4345.
6 (*a*) C. T. Ekdahl, J.-H. Claasen, S. Bonde, Z. Kokaia and O. Lindvall, *Proc. Natl. Acad. Sci. U. S. A.*, 2003, **100**, 13632; (*b*) L. Chen, H. Deng, H. Cui, J. Fang, Z. Zuo, J. Deng, Y. Li, X. Wang and L. Zhao, *Oncotarget*, 2018, **9**, 7204.
7 N. T. Zaveri, *J. Med. Chem.*, 2016, **59**, 7011.
8 N. D. Volkow and F. S. Collins, *N. Engl. J. Med.*, 2017, **377**, 391.
9 G. Yosipovitch and J. D. Bernhard, *N. Engl. J. Med.*, 2013, **368**, 1625.
10 (*a*) J. Dalli and C. N. Serhan, *Br. J. Pharmacol.*, 2019, **176**, 1024; (*b*) J. N. Fullerton and D. W. Gilroy, *Nat. Rev. Drug Discovery*, 2016, **15**, 551; (*c*) C. N. Serhan, *Nature*, 2014, **510**, 92.
11 C. N. Serhan and N. A. Petasis, *Chem. Rev.*, 2011, **111**, 5922.
12 C. N. Serhan and B. D. Levy, *J. Clin. Invest.*, 2018, **128**, 2657.
13 C. N. Serhan and N. Chiang, *Br. J. Pharmacol.*, 2008, **153**(Suppl 1), S200.
14 (*a*) W. J. Lukiw and N. G. Bazan, *Mol. Neurobiol.*, 2010, **42**, 10; (*b*) A. Asatryan and N. G. Bazan, *J. Biol. Chem.*, 2017, **292**, 12390.
15 X. Tao, M. S. Lee, C. R. Donnelly and R.-R. Ji, *Neurotherapeutics*, 2020, **17**, 886.
16 (*a*) J. R. Clapper, G. Moreno-Sanz, R. Russo, A. Guijarro, F. Vacondio, A. Duranti, A. Tontini, S. Sanchini, N. R. Sciolino, J. M. Spradley, A. G. Hohmann, A. Calignano, M. Mor, G. Tarzia and D. Piomelli, *Nat. Neurosci.*, 2010, **13**, 1265; (*b*) J. M. Walker, S. M. Huang, N. M. Strangman, K. Tsou and M. C. Sañudo-Peña, *Proc. Natl. Acad. Sci. U. S. A.*, 1999, **96**, 12198; (*c*) S. Zou and U. Kumar, *Int. J. Mol. Sci.*, 2018, **19**, 833.
17 (*a*) C. N. Serhan, S. Hong, K. Gronert, S. P. Colgan, P. R. Devchand, G. Mirick and R.-L. Moussignac, *J. Exp. Med.*, 2002, **196**, 1025; (*b*) A. Ariel, P. L. Li, W. Wang, W. X. Tang, G. Fredman, S. Hong, K. H. Gotlinger and C. N. Serhan, *J. Biol. Chem.*, 2005, **280**, 43079.
18 P. K. Mukherjee, V. L. Marcheselli, C. N. Serhan and N. G. Bazan, *Proc. Natl. Acad. Sci. U. S. A.*, 2004, **101**, 8491.
19 V. L. Marcheselli, P. K. Mukherjee, M. Arita, S. Hong, R. Antony, K. Sheets, J. W. Winkler, N. A. Petasis, C. N. Serhan and N. G. Bazan, *Prostaglandins, Leukotrienes Essent. Fatty Acids*, 2010, **82**, 27.
20 (*a*) C. N. Serhan, *FASEB J.*, 2017, **31**, 1273; (*b*) M. Perretti, *Semin. Immunol.*, 2015, **27**, 145.
21 Z.-Z. Xu, X.-J. Liu, T. Berta, C.-K. Park, N. Lü, C. N. Serhan and R.-R. Ji, *Ann. Neurol.*, 2013, **74**, 490.
22 L. Zhang, N. Terrando, Z.-Z. Xu, S. Bang, S.-E. Jordt, W. Maixner, C. N. Serhan and R.-R. Ji, *Front. Pharmacol.*, 2018, **9**, 412.
23 S. Bang, Y.-K. Xie, Z.-J. Zhang, Z. Wang, Z.-Z. Xu and R.-R. Ji, *J. Clin. Invest.*, 2018, **128**, 3568.
24 C. N. Serhan, K. Gotlinger, S. Hong, Y. Lu, J. Siegelman, T. Baer, R. Yang, S. P. Colgan and N. A. Petasis, *J. Immunol.*, 2006, **176**, 1848.
25 W. J. Guilford, J. G. Bauman, W. Skuballa, S. Bauer, G. P. Wei, D. Davey, C. Schaefer, C. Mallari, J. Terkelsen, J.-L. Tseng, J. Shen, B. Subramanyam, A. J. Schottelius and J. Parkinson, *J. Med. Chem.*, 2004, **47**, 2157.
26 (*a*) D. B. Jump, *J. Biol. Chem.*, 2002, **277**, 8755; (*b*) L. Balas, P. Risé, P. D. Gandrath, G. Rovati, C. Bolego, F. Stellari,

A. Trenti, C. Buccellati, T. Durand and A. Sala, *J. Med. Chem.*, 2019, **62**, 9961.

27 J. E. Tungen, M. Aursnes, A. Vik, S. Ramon, R. A. Colas, J. Dalli, C. N. Serhan and T. V. Hansen, *J. Nat. Prod.*, 2014, **77**, 2241.

28 J. E. Tungen, M. Aursnes, S. Ramon, R. A. Colas, C. N. Serhan, D. E. Olberg, S. Nuruddin, F. Willoch and T. V. Hansen, *Org. Biomol. Chem.*, 2018, **16**, 6818.

29 M. Aursnes, J. E. Tungen, A. Vik, R. A. Colas, C.-Y. C. Cheng, J. Dalli, C. N. Serhan and T. V. Hansen, *J. Nat. Prod.*, 2014, **77**, 910.

30 (*a*) J. Dalli, R. A. Colas and C. N. Serhan, *Sci. Rep.*, 2013, **3**, 1940; (*b*) A. Vik, J. Dalli and T. V. Hansen, *Bioorg. Med. Chem. Lett.*, 2017, **27**, 2259.

31 M. K. Pangopoulos, J. M. N. Nolsøe, S. G. Antonsen, R. A. Colas, J. Dalli, M. Aursnes, Y. Stenstrøm and T. V. Hansen, *Bioorg. Chem.*, 2020, **96**, 103653.

32 (*a*) A. Ariel, P.-L. Li, W. Wang, W.-X. Tang, G. Fredman, S. Hong, K. H. Gotlinger and C. N. Serhan, *J. Biol. Chem.*, 2005, **280**, 43079; (*b*) M. Aursnes, J. E. Tungen, R. A. Colas, I. Vlasakov, J. Dalli, C. N. Serhan and T. V. Hansen, *J. Nat. Prod.*, 2015, **78**, 2924; (*c*) K. G. Primdahl, J. E. Tungen, P. R. S. De Souza, R. A. Colas, J. Dalli, T. V. Hansen and A. Vik, *Org. Biomol. Chem.*, 2017, **15**, 8606; (*d*) K. Pistorius, P. Souza, R. Matteis, S. Austin-Williams, K. Primdahl, A. Vik, F. Mazzacuva, R. A. Colas, R. Marques, T. V. Hansen and J. Dalli, *Cell Chem. Biol.*, 2018, **25**, 749; (*e*) C. N. Serhan, K. Gotlinger, S. Hong, Y. Lu, J. Siegelman, T. Baer, R. Yang, S.-P. Colgan and N. A. Petasis, *J. Immunol.*, 2006, **176**, 1848; (*f*) N. A. Petasis, R. Yang, J. W. Winkler, M. Zhu, J. Uddin, J. N. G. Bazan and C. N. Serhan, *Tetrahedron Lett.*, 2012, **53**, 1695; (*g*) A. R. Rodrigues and B. W. Spur, *Tetrahedron Lett.*, 2014, **55**, 6011.

33 (*a*) F. Frigerio, G. Pasqualini, I. Craparotta, S. Marchini, E. A. van Vliet, P. Foerch, C. Vandenplas, K. Leclercq, E. Aronica, L. Porcu, K. Pistorius, R. A. Colas, T. V. Hansen, M. Perretti, R. M. Kaminski, J. Dalli and A. Vezzani, *Brain*, 2018, **141**, 3130; (*b*) T. Gobbetti, J. Dalli, R. A. Colas, D. F. Canova, M. Aursnes, D. Bonnet, L. Alric, N. Vergnolle, C. Deraison, T. V. Hansen, C. N. Serhan and M. Perretti, *Proc. Natl. Acad. Sci. U. S. A.*, 2017, **114**, 3963; (*c*) Y. Tian, M. Aursnes, T. V. Hansen, J. E. Tungen, J. D. Galpin, L. Leisle, C. A. Ahern, R. Xu, S. H. Heinemann and T. Hoshi, *Proc. Natl. Acad. Sci. U. S. A.*, 2016, **113**, 13905; (*d*) T. V. Hansen, J. Dalli and C. N. Serhan, *Prostaglandins Other Lipid Mediators*, 2017, **133**, 103; (*e*) K. G. Primdahl, J. E. Tungen and T. V. Hansen, *J. Nat. Prod.*, 2020, **83**, 2255.

34 M. Aursnes, J. E. Tungen, A. Vik, J. Dalli and T. V. Hansen, *Org. Biomol. Chem.*, 2014, **12**, 432.

35 J. E. Tungen, M. Aursnes, J. Dalli, H. Arnardottir, C. N. Serhan and T. V. Hansen, *Chem. – Eur. J.*, 2014, **20**, 14575.

36 (*a*) J. Becher, *Org. Synth.*, 1979, **59**, 79; (*b*) J. M. J. Nolsøe, M. Aursnes, J. E. Tungen and T. V. Hansen, *J. Org. Chem.*, 2015, **80**, 5377.

37 F. Näf, R. Decorzant, W. Thommen, B. Willhalm and G. Ohloff, *Helv. Chim. Acta*, 1975, **58**, 1016.

38 B. C. Callaghan, H. T. Cheng, C. L. Stables, A. L. Smith and E. L. Feldman, *Lancet Neurol.*, 2012, **11**, 521.

39 H. Field, J. Gao, P. Motwani and H. K. Wong, *Dermatol. Ther.*, 2016, **6**, 579.

40 Q. Han, D. Liu, M. Convertino, Z. Wang, C. Jiang, Y. H. Kim, X. Luo, X. Zhang, A. Nackley, N. V. Dokholyan and R.-R. Ji, *Neuron*, 2018, **99**, 449.

41 Y. Kawasaki, Z.-Z. Xu, X. Wang, J. Y. Park, Z.-Y. Zhuang, P.-H. Tan, Y.-J. Gao, K. Roy, G. Corfas, E. H. Lo and R.-R. Ji, *Nat. Med.*, 2008, **14**, 331.

42 M. Wernerova and T. Hudlicky, *Synlett*, 2010, 2701.

43 J. E. Tungen, M. Aursnes and T. V. Hansen, *Tetrahedron Lett.*, 2015, **56**, 1843.

44 Z.-Z. Xu, T. Berta and R.-R. Ji, *J. Neuroimmune Pharmacol.*, 2013, **8**, 37.

45 W. J. Dixon, *Annu. Rev. Pharmacol. Toxicol.*, 1980, **20**, 441.

46 S. Chandra, Z. Wang, X. Tao, O. Chen, X. Luo and R.-R. Ji, *Anesthesiology*, 2020, **133**, 611.